THE UNIVERSITY OF TEXAS AT AUSTIN
DEPARTMENT OF AEROSPACE ENGINEERING AND ENGINEERING MECHANICS

EM 388F – Fracture Mechanics
Professor: Dr. Rui Huang

Theory and analysis techniques for the use of a DCB specimen for determining the toughness of PC-3 Prostate Cancer

Justin Babcock
May 7, 2008

Term Paper

1. Abstract

A double cantilever beam (DCB) specimen is created by affixing the two halves together using a bi-layer of PC-3 prostate cancer cells. The specimen is pinned at a bottom corner, and the upper corner on the same end is displaced with the force-displacement profile being recorded. This upper corner is displaced until the crack, a portion of the specimen where cell growth has been selectively inhibited, propagates through the cell layer. The critical value of force at which the crack propagates through the cell layer is used, in conjunction with the initial crack length, to determine the toughness via the compliance-energy method (Ripling, Mostovoy, et al. 1971). A method for performing a FE analysis of the specimen is developed with increasing complexity. The basic model involves computing the J-integral (Rice 1968) on a finite element model to which the predicted critical value of force has been applied. The first extension of this basic method involves modeling the cell layer as a spring foundation, applying a predetermined critical force, and computing the J-integral (Song 1994). The final enhancement involves the use of a traction-separation law for the cells through the use of cohesive elements in a F.E. model. The traction-separation law is determined by experimental work. This model is then used to determine the critical value of force and toughness via the J-integral.

2. Introduction

Metastasis, the process in which cancer cells detach from a primary tumor and migrate to secondary sites within the body forming secondary tumors, is partially dependent, on detachment and adhesion (Weiss 2000a). Primary tumors, which are often manageable by removal or some other form of localized treatment, contrast with these secondary tumors or metastases which are nearly always fatal.

A further understanding of the process of metastasis should lead to an increased ability to prevent it from happening. Cancer cell adhesion is thought to be an important factor in the process of metastasis as it relates to the release and arrest of cancer cells from the primary tumor (Weiss 2000b). There are many different factors affecting cell adhesion. Further, there are many different issues to be addressed; the mechanisms of attachment and detachment, the modeling of these mechanisms, the mechanical properties of adhesion, etc. This paper investigates a mechanical property; toughness. Given that the cancer cells detach from other cancer cells on the primary tumor, the use of toughness as an adhesion property seems logical.

In this paper an experimental setup for investigating the toughness of a PC-3 prostate cancer cells is outlined. A method for modeling the experiment is described, with increasing levels of sophistication that progressively allow for a more accurate simulation.

3. Experimental

3.1. PC-3 Cell line background

The initial establishment of the PC-3 cell line is described in detail in (Kaighn, Shankar Narayan et al. 1979). The PC-3 cell line was created from metastatic tumor tissue discovered in the bone marrow from the lumbar vertebra of a 62 year old male subject. This secondary tumor had originated from a primary tumor in the prostate, as confirmed by a prostatic biopsy that "revealed poorly differentiated prostatic adenocarinoma"."

3.2. Specimen

A rendering of the actual specimen is seen in Figure 1. The increased width section, referred to as the tab, allows for the attachment of the specimen to the test fixture. The two halves are cut from larger microscope slides and then assembled. They are then cleaned, plasma treated, and then placed in a Petri dish containing the cells and a growth media. An area that is referred to as the initial crack is masked so that cells do not grow on the surface. When the cells have created a confluent monolayer, the is masking removed, and the two halves are brought together in the media. They are allowed to bond together for 6 hours. The specimen is then mounted in the test apparatus, submerged in growth media to negate the effects of surface tension, and the experiment carried out. The experiment is repeated many times and at different initial crack lengths to allow for determination of the derivative of compliance with respect to crack length, a required piece of data.

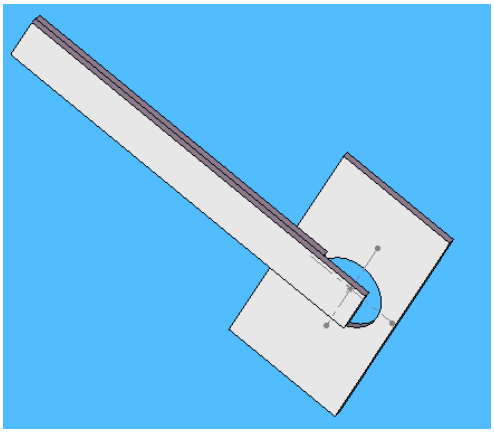

Figure 1 – Cell toughness testing specimen

Figure 2 shows the basic model of the specimen. It also highlights the basic elements of the experiment such the initial crack length, a_o, the pin attachment at the lower left corner the force, P, and displacement, Δ. The instantaneous crack length, a, and the bridging zone length, α, will come into consideration in the third modeling technique that considers crack extension through use of a traction-separation law for the cells.

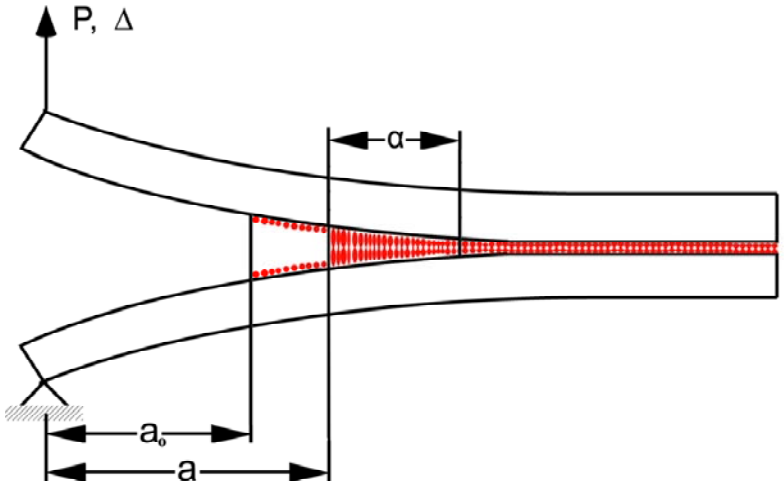

Figure 2 – Model of specimen

3.3. Setup

An overall view of the test apparatus, along with a close up of the specimen mounting, can be seen in Figure 3. Without going into extreme detail, the basic mechanics are as follows. A linear motor pushes on a load cell that then pushes a platform that is suspended from four leaf springs. This displaced platform then pushes on the specimen. The force required to separate the specimen is recorded by the load cell, and the displacement of the specimen is recorded locally by a DVRT.

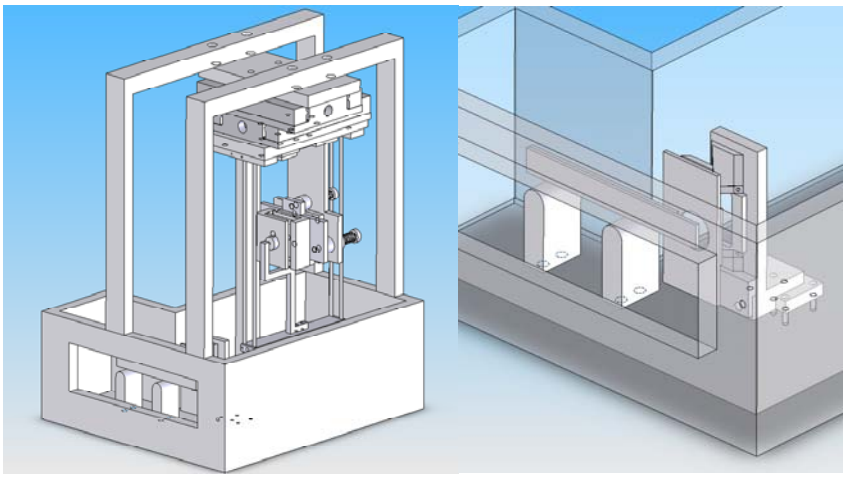
Figure 3 – Test apparatus with close-up of specimen mount

4. Several modeling methods

Soft biological tissues are viscoelastic, inhomogeneous, anisotropic and are often subjected to large deformations. Understandably, a model that encompasses all of these properties is necessarily very complex. The basic model and its improvements described

herein is a simplification of reality. On the simplest level, section 4.1, the deformation of the specimen due to the cell layer is not even accounted for. At the next level of complexity, section 4.2, this displacement is accounted for by modeling the layer as springs. At the highest level of complexity considered, section 4.3, the failure of cell-cell bonds is accounted for which allows for a simulation of crack propagation.

4.1. Basis model – Solid DCB, Finite element model thereof

The basic approach for this basic model is outlined in (Ripling, Mostovoy et al. 1971). The specimen is considered to be a solid object with no adhesive layer. Thus the deformation of the adhesive is not taken into account when determining G_c, P_c, or Δ_c. This is a fundamental limitation of this basic model, though it does produce reasonable results. Errors are approximately on the order of 10%.

It can be shown that the energy release rate G can be expressed as

$$G = -\frac{\partial \Pi}{\partial A} \tag{1}$$

where Π is the potential energy of deformation, equation 2, and A is the crack surface area.

$$\Pi = U - P\Delta \tag{2}$$

U is the strain energy as given in equation 3.

$$U = \frac{1}{2} P\Delta \tag{3}$$

Now substituting equations 2 and 3 into equation 1, we arrive at equation 4.

$$G = \frac{P}{2b}\left(\frac{d\Delta}{da}\right)_P \tag{4}$$

where b is the thickness and a the crack length so that the product of a and b is the area A. Now we substitute equation 5 into equation 4 and we arrive at equation 6.

$$C = \frac{\Delta}{P} \tag{5}$$

$$G = \frac{P^2}{2b}\frac{dC}{da} \tag{6}$$

Equation 6 will be used when conducting experiments in order to determine G. It should be noted that this implies that multiple experiments will need to be under taken so that a dC/da relationship can be established. Reliance on a theoretical value could be problematic as the actual behavior might be different enough to significantly affect the resulting value of G.

It is possible to establish an expression for G solely in terms of material properties and geometry given the theoretical model assumptions. This formulation allows us to predict P_c and Δ_c for a given G_c. Using order of magnitude values for G_c, available from other studies undertaken on similar cancer cells, it is possible to design the specimen and determine the P_c and Δ_c, both of which are necessary parameters for the design of the test apparatus. Equations 7, 8, and 9 are the resulting necessary equations.

$$G_c = \frac{12P_c^2a^2}{b^2h^3E} \tag{7}$$

$$P_c = \sqrt{\frac{G_cb^2h^3E}{12a^2}} \tag{8}$$

$$\Delta_c = \frac{8P_ca^3}{Ebh} \tag{9}$$

As part of this implementation, a finite element model of the specimen is constructed in order that a second method can be used to determine G_c. A basic solid form with specified geometry and crack of length a is constructed in any finite element program capable of calculating the J integral (Rice 1968). Either equations 8 or 9 or experimental data is used as the basis for a critical force or displacement. This critical load or displacement is then applied to the model. The J integral is then performed on appropriate contours, with the avoidance of stress concentrations being the main concern. Figure 4 shows the deformed model having had the critical load for a given crack length and G_c applied. The resulting value of the J integral is then compared to the analytical solution for G_c. Theoretically they should agree. The closer the two are in value the more confidence can be put into the answer for G_c.

Figure 4 – Deformed FE model of specimen with von Mises stress field superimposed

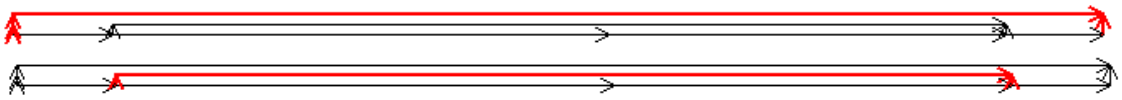

Figure 5 – J integral paths. Top is path 1, bottom is path 2

Figure 6 provides a comparison of results for a sample FE model. The value of K_c is related to G_c via equation 10. The J integral is the taken along paths 1 and 2 (see Figure 5) and its values converted from G to K again using equation 10. Note that as long as a "good" path is chosen, the J integral provides a value of K that is very close to the theoretical value.

$$J = G_c = \left(K_{IC}\right)^2 \frac{(1-\nu^2)}{E} \qquad (10)$$

where E is the Young's modulus and ν the Poison's ratio.

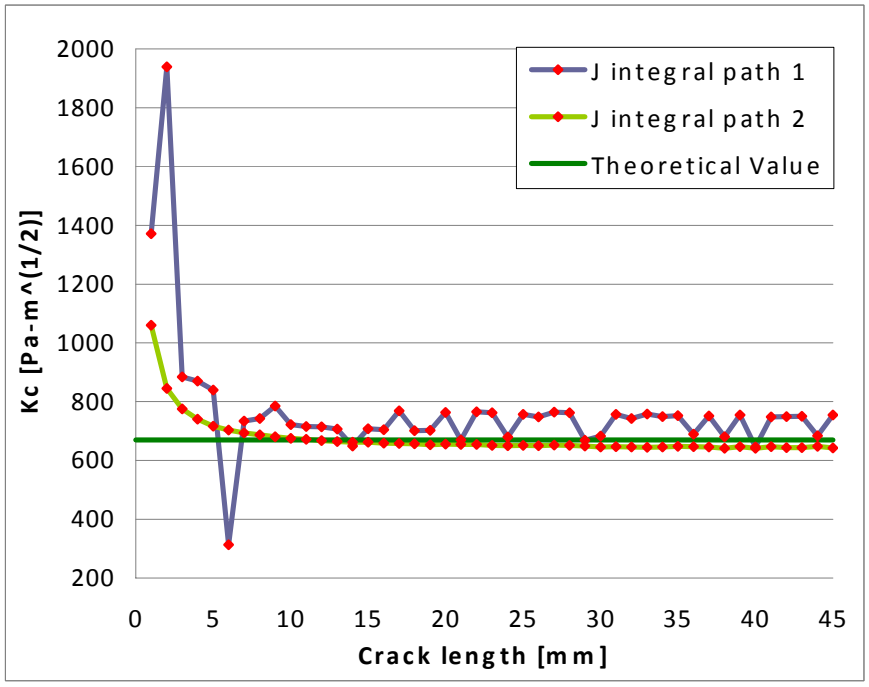

Figure 6 – K_c calculated using two paths for J integral

Though satisfactory FE models that simulate this model can be constructed rather simply, this basic implementation doesn't take into account the rotations and displacements of the specimen that will arise due to the deformation of the cell layer. For this a greater level of complexity is required and is addressed in section 4.2.

4.2. Extended model, Spring foundation

The basics of this model are outlined in (Song 1994). The specific application discussed is for a delamination failure of laminated composites. Advantageously though, the model developed for calculating G_c is an extension of our basic DCB model. Instead of neglecting the presence of the adhesive layer, it is modeled as a non-linear spring foundation. Thus the deflection and rotation of the tip due to the adhesive is accounted for. Figure 7 shows the specimen and the model of the specimen.

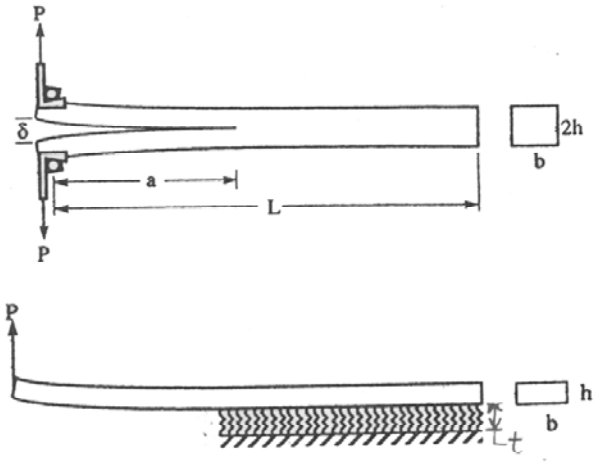

Figure 7 – Method II model, adapted from (Song 1994)

The constitutive laws for the spring and beam are given in equations 11 and 12 respectively. In the specific case discussed in the reference, the spring foundation is modeled as non-linear, though there is no reason why another type couldn't be used.

$$\sigma_m = \alpha\left(1 - e^{-\beta\varepsilon_m}\right) \qquad 0 \le z \le t \tag{11}$$

$$\sigma_p = E_p\varepsilon_p \qquad t \le z \le h \tag{12}$$

where t is the thickness of the adhesive layer and h the thickness of the specimen.

The onset of crack propagation is based on an energy criterion, G_c. Equation 1 is perfectly valid for this model so an expression is developed for Π, equation 13.

$$\Pi = U_{Beam} + U_{Spring} - W_e \tag{13}$$

where U_{Beam} and U_{Spring} are the strain energy of the beam and spring and W_e the external work potential, analogous to the –PΔ term in equation 2.

The general form of strain energy is given in equation 14.

$$U = \int_0^h \int_0^\varepsilon \sigma d\varepsilon dz \tag{14}$$

When the first integration, with respect to strain, is undertaken for the case outlined in the reference, the resulting equation is 15.

$$U_{Spring} + U_{Beam} = \int_0^t \alpha \left(\varepsilon_m + t_i \frac{1}{\beta} \left(e^{-\beta \varepsilon_m} - 1 \right) \right) dz + \int_t^h \frac{1}{2} E_p \varepsilon_p^2 dz \qquad (15)$$

With a model of the strain energy, an equation for critical energy release rate can be formulated using equation 1. The deflections upon which the strains and stresses are based must be calculated using a finite element implementation, iterating values of P until G_c is reached. In the reference, a FE code is written, though commercially available codes are available that could be used as well. The main consideration is that spring elements can be defined with specific constitutive properties.

In addition to this equation 1 approach towards formulating a value of G, the J-integral method can be used. The use of this method is recommended as it provides a check of the implemented method. An agreement, or at least very close match, between the two methods provides a check and increases confidence in the results. As in section 4.1, care should be taken to choose a satisfactory integration path that avoids trouble areas such as stress concentrations.

As failure, the onset of crack propagation, is determined using an energy criterion it follows that a G_c must be either supplied or calculated. In the case of this model, G_c or P_c and Δ_c must be provided. In the reference a G_c of the adhesive was provided. If however a P_c and Δ_c were determined from experiments it should be possible to apply these to the FE model and then calculate the G_c. So although the model is versatile in this respect, and in that it accounts for the additional rotation and displacement effects of the cell layer, it cannot calculate a G_c, P_c and Δ_c simultaneously. This is capability is addressed in the final extension of our model in section 4.3.

4.3. Final model – Traction-separation law, cohesive elements

In this final revision of the model, the cells are modeled by a traction-separation law that is analogous to the spring model previously mentioned, but in terms of a displacement, not a strain. Further, it is set apart by a failure criterion for the cell-cell bonds; a critical displacement.

This traction-separation law for the PC-3 is something that must be determined from testing, or arrived at by starting with a good working knowledge of similar cell's traction-separation behavior. With knowledge of other similar cell's behavior, it would be possible to tweak the specifics of the law until a model is arrived at that accurately simulates the experimental results.

As described in (Bao and Suo 1992) the basic form of a traction-separation law is given in equation 16.

$$\frac{\sigma}{\sigma_o} = \chi \left(\frac{\delta}{\delta_o} \right) \qquad (16)$$

where σ is the applied stress, σ_o the strength of the bond, δ the applied separation, δ_o the critical value of separation and χ a function that gives the shape of the relationship (which is arbitrary) as seen in Figure 8.

The model is now specified as a FE beam with a single layer of cohesive elements within abaqus. The specifics of the traction-separation law are coded into the cohesive elements. The deformation of these elements accounts for the displacement and rotation due to the layer of cells in the same way as did the springs. One improvement of this model is the ability to predict a P_c and a Δ_c without being given a G_c.

An additional benefit of this model is its ability to predict not only critical force and separation but also critical energy release rate. By taking a J-integral over an appropriate path, as previously discussed, G at the state of P_c and Δ_c can be calculated, which is by definition G_c.

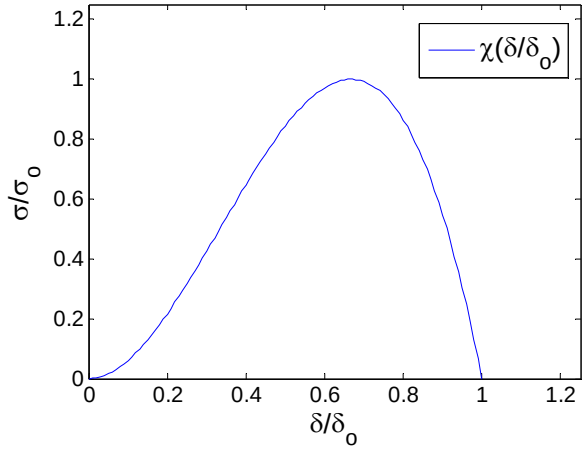

Figure 8 – Plot of traction-separation law, adapted from (Bao and Suo 1992)

Another big improvement is the ability to model the crack propagation behavior. The main benefit of this, and for that matter a driving purpose for comparing experimental results to numerical simulation results, is to have a way of backing up experimental results. If it is possible to model the behavior in a way that goes beyond simply fitting a curve to the data then the confidence in the results is immensely boosted.

5. Conclusion

In expanding upon the basic model, an additionally complex and better method is developed that more closely models the real situation. Having a theoretical model that agrees well with experimental results bolsters ones confidence in the results and the model. Seeing an improvement in agreement as complexity increases is also a good sign that the aspects being added to the model are brining it closer and closer to a reality.

The motivation for the use of the methods described herein has been detailed. By understanding the adhesion properties of cancer, our understanding of metastasis will be furthered. This understanding will hopefully lead to metastasis's highly deadly effects being avoided or at least minimized.

6. References

Bao, G. and Z. Suo (1992). "Remarks on crack-bridging concepts." Applied Mechanics Reviews **45** (8): pp. 355-366.

Kaighn, M. E., K. Shankar Narayan, et al. (1979). "Establishment and characterization of a human prostatic carcinoma cell line (PC-3)." Investigative Urology **17**(1): 16 - 23.

Rice, J. R. (1968). "A path independent integral and the approximate analysis of strain concentration by notches and cracks." ASME Journal of Applied Mechanics **35**: 379-386.

Ripling, E. J., S. Mostovoy, et al. (1971). "Fracture Mechanics: A Tool for Evaluating Structural Adhesives." Adhesion **3**(2): 107 - 123.

Song, S. J., Waas, A. M. (1994). "A spring foundation model for mode I failure of laminated composites based on an energy criterion." J. Eng. Mater. Technol. (Trans. ASME) **116**(4): 512-516.

Weiss, L. (2000a). "Introduction." Cancer and Metastasis Reviews **19**(3): 8-10.

Weiss, L. (2000b). "Some Cell Interactions." Cancer and Metastasis Reviews **19**(3): 235-255.